Dominant Pole Localization of FxLMS Adaptation Process in Active Noise Control

Iman Tabatabaei Ardekani, Waleed H. Abdulla
The University of Auckland, Private Bag 92019, Auckland, New Zealand

***Abstract*—This paper develops a technique for dominant pole localization of the adaptation process, performed by the FxLMS algorithm in active noise control systems. This development results in a new adaptation algorithm, called Filtered Weight FxLMS (FwFxLMS). Similar to the FxLMS, FwFxLMS uses a recursion for updating the weight vector of a transversal ANC controller. However, in the new algorithm, the weight vector is filtered before being updated by the recursion. This filtering procedure causes dynamic behaviors of the adaptation process to be improved. This improvement can be theoretically proved by plotting and analyzing the root locus of the adaptation process in the z-plane. Also, simulation results show the efficiency of the proposed algorithm in active control of acoustic noise.**

I. Introduction

Active control of acoustic noise, usually referred to as Active Noise Control (ANC), relies on the simple concept that the combination of two acoustic waves with equal magnitudes but opposite phases makes silence at the conjunction point; consequently, in a neighborhood of the conjunction point, a silence zone is created. However, only with the advent of digital technology, did the design and implementation of adaptive ANC systems become possible. The idea of adaptive ANC was published in 1975 [1]. Shortly after, different structures for realization of this theory were developed [2]–[5]. Usually, these structures consist of an acoustic data acquisition system, a DSP processor and an adaptation algorithm. This algorithm, itself, consists of the following two processes.

1) An estimation process for generating an anti-noise signal.
2) An adaptation process for automatic adjustment of the parameters used in the estimation process.

Usually, a transversal filter is used for performing the estimation process. In ANC literature, this filter is called the ANC controller [6], [7]. Also, an adaptation algorithm is used for performing the adaptation process on the weight vector of the ANC controller. This algorithm is responsible for the automatic adjustment of the ANC controller such that the combination of environmental noise and anti-noise at a desired silence zone is minimized. The most popular ANC adaptation algorithm, called Filtered-x Least-Mean-Square (FxLMS) was proposed by Widrow in 1981 [8]. The main advantage of this algorithm is its simplicity; however, it has slow dynamics.

The main objective of this paper is to modify the FxLMS algorithm in order to improve its dynamic behavior. This modification leads to develop a new adaptive algorithm, called Filtered Weight FxLMS. The rest of this paper is organized as follows. Section 2 introduces the FxLMS-based ANC and describes the FxLMS root locus, based on the authors previous work [9], [10]. Section 3 modifies the FxLMS algorithm and determines influences of the proposed modification on the FxLMS root locus. It is then shown that the dominant pole of the adaptation process can be localized by adjusting the proposed modification. This ability enable us to make the adaptation process faster. Section 4 shows the validity of the theoretical results using computer simulation. Finally, Section 5 gives concluding remarks.

II. FxLMS-Based Active Noise Control

The functional block diagram of the FxLMS-based ANC system is illustrated in Figure 1. In this diagram, transfer functions $P(z)$ and $S(z)$ represent primary and secondary paths (or systems), respectively. These two linear systems are unknown electro-acoustic channels with finite impulse responses. As shown, the FxLMS algorithm adjusts the ANC controller weight vector in accordance with the residual acoustic noise signal $e(n)$ and the reference signal $x(n)$, picked up by two separate microphones. Referring to the diagram, electrical signal $e(n)$ can be expressed as

$$e(n) = d(n) - \sum_{q=0}^{Q-1} s_q \mathbf{w}^T(n-q)\,\mathbf{x}(n-q), \qquad (1)$$

where scalar parameters $s_0, s_1, \ldots, s_{Q-1}$ are coefficients of the secondary path impulse response, $\mathbf{x}(n)$, called the reference vector, is the $L \times 1$ tap vector of the reference signal $x(n)$:

$$\mathbf{x}(n) = \begin{bmatrix} x(n) & x(n-1) & \ldots & x(n-L+1) \end{bmatrix}^T \qquad (2)$$

and $\mathbf{w}(n)$, called the weight vector is given by

$$\mathbf{w}(n) = \begin{bmatrix} w_0(n) & w_1(n) & \ldots & w_{L-1}(n) \end{bmatrix}^T \qquad (3)$$

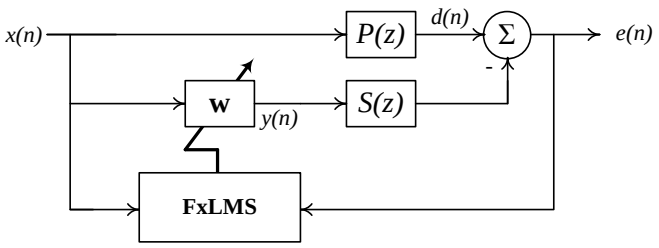

Figure 1. Functional block diagram of FxLMS-based ANC system

The FxLMS algorithm updates $\mathbf{w}(n)$ by using the following recursive equation at time index n .

$$\mathbf{w}(n+1) = \mathbf{w}(n) + \mu e(n) \underbrace{\sum_{q=0}^{Q-1} s_q \mathbf{x}(n-q)}_{\mathbf{x}_f(n)}, \tag{4}$$

where scalar parameter μ is the adaptation step-size and $\mathbf{x}_f(n)$ is the filtered reference vector, obtained by filtering $\mathbf{x}(n)$ using an estimate of the secondary path, called the secondary path model. In practice, this model can be estimated using off-line or on-line secondary path modeling techniques [6]. Usually, it can be assumed that the secondary path model is identical to the actual secondary path.

A. FxLMS Characteristic Equation

In [11], it is shown that for a broad-band white acoustic noise of power σ_x^2, the variation of the first order moment of the weight vector $\mathbf{w}(n)$ can be modeled as

$$\overline{\mathbf{c}}(n+1) = \overline{\mathbf{c}}(n) - \mu\sigma_x^2 \sum_{q=0}^{Q-1} s_q^2 \overline{\mathbf{c}}(n-q) \tag{5}$$

where $\overline{\mathbf{c}}(n)$ is the first order moment of $\mathbf{w}(n)$, defined as

$$\overline{\mathbf{c}}(n) \triangleq E\{\mathbf{w}(n) - \mathbf{w}_{opt}\} \tag{6}$$

In this model, constant vector $\mathbf{w}_{opt}$ denotes the optimum Wiener–Hopf solution and operator $E\{.\}$ denotes the statistical expectation. Taking the z-transform from Eq. (5), the FxLMS characteristic equation can be obtained as

$$z - 1 + \mu\sigma_x^2 \sum_{q=0}^{Q-1} s_q^2 z^{-q} = 0 \tag{7}$$

This equation can be expressed in the standard form of

$$1 + \mu\sigma_x^2 H(z) = 0 \tag{8}$$

where $H(z)$, called the FxLMS open loop transfer function, is defined as

$$H(z) = \frac{\sum_{q=0}^{Q-1} s_q^2 z^{Q-1-q}}{z^Q - z^{Q-1}} \tag{9}$$

B. FxLMS Root Locus

Since the FxLMS characteristic equation, given in Eq. (8), is a parametric polynomial equation of order Q (with scalar parameter μ), finding closed-loop expressions for its roots is impossible in mathematics. However, the authors derived the rules governing on the root locus of this equation in [10] and [9]. In the following these rules are briefly described.

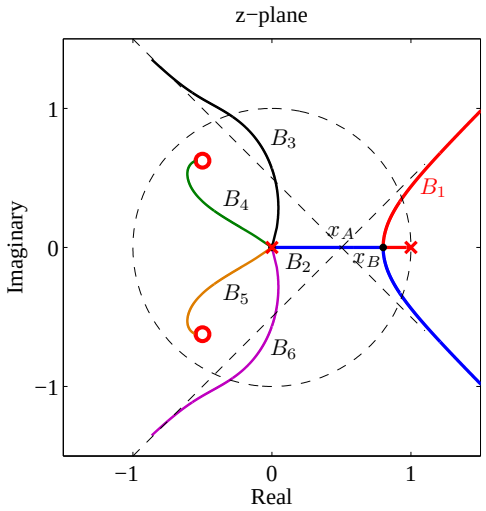

Figure 2. An example for FxLMS root locus when $s_0 = s_1 = s_2 = 0$, $s_3 = s_4 = 1$ and $s_5 = 0.8$ ($Q = 6$).

Number of Branches : the FxLMS root locus has Q branches, denoted by $B_1, B_2, ...$and B_Q. As a particular example, for the secondary path impulse response, given by parameters $s_0 = s_1 = s_2 = 0$, $s_3 = s_4 = 1$ and $s_5 = 0.8$, the FxLMS root locus contains 6 distinct branches (because $Q = 6$). For this example, the open loop transfer function $H(z)$ can be computed as

$$H(z) = \frac{z^2 + z + 0.8}{z^6 - z^5} \tag{10}$$

Trajectories of these branches in the z-plane are computed in MATLAB and then plotted in Figure 2.

Start Points : the start point of B_1 locates at $z = 1$ and those of $B_2, B_3, ...$ and B_Q locate at the $z = 0$, commonly. These points are marked in Figure 2 by "x".

End Points: end points of $B_1, B_2, ...$and B_Q locate at the zeros of $H(z)$. Unlike start points, end points are not constants and their location is a function of secondary path coefficients squares $s_0^2, s_1^2, \ldots,$ and s_{Q-1}^2. Accordingly, end points of the FxLMS root locus can not be given in closed-form expressions. However, it is obvious from Eq. (9) that the number of zeros of $H(z)$ can be less than the number of branches (that is Q). This is because, the first coefficients of the secondary path are likely to be zero, due to the existence of a time delay in in the secondary path. Assuming that the first Q_0 coefficients of the secondary path are zero ($s_0 = s_1 = \ldots = s_{Q_o-1} = 0$), $H(z)$ can have only $Q - Q_0 - 1$ finite zeros. This is while the FxLMS root locus has Q separate branches in the z-plane. In this case, the branches for excess poles approach one asymptote each.
For the example described above, the three first coefficients of the secondary path impulse response are zero ($Q_0 = 3$). Consequently, $H(z)$ have only 2 finite zeros at which two branches of the root locus can end. These points are shown in Figure 2 by "o". As can be seen, B_4 and B_5 ends at these points. The other 4 branches approach infinity along with 4 distinct asymptotes of the root locus.

Asymptotes: according to the root locus theory, the number of asymptotes in a root locus is equal to the difference between the number of poles and zeros of the open loop transfer function $H(z)$. Accordingly, the FxLMS root locus has Q_0+1 asymptotes. In [9], it is shown that these asymptotes originate on the real axis at the centroid point x_A, given by

$$x_A = \frac{1 + \left(\frac{s_{Q_0+1}}{s_{Q_0}}\right)^2}{Q_0 + 1} \tag{11}$$

and form angles with respect to the real axis of

$$\varphi_k = \frac{(2k+1)}{Q_0+1}\pi \qquad k = 0, 1, ..., Q_0 \tag{12}$$

For the example described above, x_A can be obtained by setting $Q_0 = 3$, $s_{Q_0} = s_3 = 1$ and $s_{Q_0+1} = s_4 = 1$ in Eq. (11) as $x_A = \frac{1}{2}$. Also, the angles of the 4 asymptotes can be obtained by setting $Q_0 = 3$ in Eq. (12) as $\varphi_1 = \frac{\pi}{4}$, $\varphi_2 = \frac{3\pi}{4}$, $\varphi_3 = \frac{5\pi}{4}$ and $\varphi_4 = \frac{7\pi}{4}$. The centroid point at $x_A = \frac{1}{2}$ and the 4 asymptotes, specified above, are shown in Figure 2. As can be seen, B_1, B_2, B_3 and B_6 approach these asymptotes.

Departure Angles: the departure angle of the FxLMS root locus branches from their start points are given by

$$\theta_q = \begin{cases} \pi, & q = 1 \\ \frac{2(q-2)}{Q-1}\pi, & q = 2, 3, ..., Q \end{cases} \tag{13}$$

For the example, described above, departure angles can be computed by setting $Q = 6$ in Eq. (13) as $\theta_1 = \pi$, $\theta_2 = 0$, $\theta_3 = \frac{2\pi}{5}$, $\theta_4 = \frac{4\pi}{5}$, $\theta_5 = \frac{6\pi}{5}$ and $\theta_6 = \frac{8\pi}{5}$.

Real Sections: an interval on the real axis belongs to the FxLMS root locus if $H(z)$ has an odd number of zeros and poles to its right. Since all nominator coefficients of $H(z)$ are positive, $H(z)$ can only have complex conjugate zeros to the right of the imaginary axis. Besides, $H(z)$ has a single pole at $z = 1$. Therefore the only interval of the positive real axis which belongs to the FxLMS root locus is $(0, 1)$.

Breakaway Points: the most important breakaway point in the FxLMS root locus locates at the real axis between $(0, 1)$. The location of this point is given by [10]

$$x_B = \frac{D_{eq}}{D_{eq} + 1} \tag{14}$$

where D_{eq} is defined as

$$D = \frac{\mathbf{s}^T \mathbf{\Psi} \mathbf{s}}{\|\mathbf{s}\|^2} \tag{15}$$

and

$$\mathbf{\Psi} = diag(0, 1, \ldots, Q-1) \tag{16}$$

For the example, described above, D_{eq} can be computed as $D_{eq} = 3.86$. Setting this value in Eq. (14) results in $x_B = 0.79$. The location of this point is shown in Figure 2.

C. Typical Trajectories of FxLMS Root Locus

From the rules described above, it can be deduced that B_1 always starts at $z = 1$ and moves towards the origin on the real axis. This branch leaves the real axis and detours towards the unit circle once reaching the breakaway point x_B. Also, it can be deduced that B_2 starts at $z = 0$ and moves towards the unit circle on the positive real axis. This branch leaves the real axis once reaching the breakaway point x_B in such a way that points of this branch remain complex conjugates of those of B_1. Other branches ($B_3, B_4, \ldots,$ and B_Q) always start at $z = 0$ (with different departure angles) and moves towards the unit circle in order to end at the zeros of $H(z)$ or approach the asymptotes.

Based on these typical trajectories in the FxLMS root locus, it is expected that the nearest root to the unit circle locates on B_1. Therefore, this branch always contains the dominant root of the FxLMS characteristic equation. As a conclusion, if a mechanism can push this root towards the origin, the dynamic of the first order moment $\bar{\mathbf{c}}(n)$ becomes faster. This is the key idea for the development of the algorithm, proposed in the following section.

III. Filtered Weights FxLMS Algorithm

The update equation of the proposed adaptation algorithm, called the Filtered Weights FxLMS (FwFxLMS) is given by

$$\mathbf{w}(n+1) = \mathbf{w}_a(n) + \mu e(n) \sum_{q=0}^{Q-1} s_q \mathbf{x}(n-q) \tag{17}$$

where $\mathbf{w}_a(n)$, called the filtered weight vector, is obtained by passing the weight vector $\mathbf{w}(n)$ through a recursive filter with the transfer function given by

$$A(z) = \frac{1-\xi}{1-\xi z^{-1}} \tag{18}$$

The reason behind the current form of $A(z)$ will become apparent, later. Obviously, internal stability of $A(z)$ requires $-1 < \xi < 1$; however, at this stage, it is assumed that ξ is positive; therefore,

$$0 < \xi < 1 \tag{19}$$

Assuming that $a(n)$ is the inverse z-transform of $A(z)$, the filtered weight vector $\mathbf{w}_A(n)$ can be expressed as

$$\begin{aligned} \mathbf{w}_a(n) &\triangleq a(n) * \mathbf{w}(n) \\ &= \mathbf{w}(n) - \xi[\mathbf{w}(n) - \mathbf{w}_a(n-1)] \end{aligned} \tag{20}$$

Now, it is required to express the proposed updating equation in terms of the misalignment weight vector. For this purpose, both sides of Eq. (17) is modified to

$$\mathbf{w}(n+1) - \mathbf{w}_{opt} = \mathbf{w}_a(n) - \mathbf{w}_{opt} + \mu e(n) \sum_{q=0}^{Q-1} s_q \mathbf{x}(n-q) \tag{21}$$

Now, by defining the misalignment weight vector as

$$\mathbf{c}(n) = \mathbf{w}(n) - \mathbf{w}_{opt} \tag{22}$$

Eq. (21) can be re-expressed as

$$\mathbf{c}\left(n+1\right)=\mathbf{w}_{a}\left(n\right)-\mathbf{w}_{opt}+\mu e\left(n\right)\sum_{q=0}^{Q-1}s_{q}\mathbf{x}\left(n-q\right) \quad (23)$$

On the other hand, it can be shown from Eq. (20) that

$$\begin{aligned}\mathbf{w}_{a}\left(n\right)-\mathbf{w}_{opt} &= \left[\mathbf{w}\left(n\right)-\mathbf{w}_{opt}\right]-\xi\left[\mathbf{w}\left(n\right)-\mathbf{w}_{opt}\right.\\ &\quad\left.-\mathbf{w}_{a}\left(n-1\right)+\mathbf{w}_{opt}\right] \quad (24)\end{aligned}$$

Now, substituting Eq. (22) into (24) results in

$$\mathbf{w}_{a}\left(n\right)-\mathbf{w}_{opt}=\mathbf{c}\left(n\right)-\xi\left[\mathbf{c}\left(n\right)-\left(\mathbf{w}_{a}\left(n-1\right)+\mathbf{w}_{opt}\right)\right] \quad (25)$$

Based to the definition given in Eq. (20), it can be shown from Eq. (25) that

$$\mathbf{w}_{a}\left(n\right)-\mathbf{w}_{opt}=a\left(n\right)*\mathbf{c}\left(n\right) \quad (26)$$

Finally, substituting Eq. (26) into (23) gives

$$\mathbf{c}\left(n+1\right)=a\left(n\right)*\mathbf{c}\left(n\right)+\mu e\left(n\right)\sum_{q=0}^{Q-1}s_{q}\mathbf{x}\left(n-q\right) \quad (27)$$

which gives an alternative expression for the FwFxLMS update equation.

A. FwFxLMS Characteristic Equation

By taking the statistical expectation from both sides of Eq. (27) and after applying the same logic used in [11] for the derivation of Eq. (5), it can be shown that

$$\overline{\mathbf{c}}\left(n+1\right)=a(n)*\overline{\mathbf{c}}\left(n\right)-\mu\sigma_{x}^{2}\sum_{q=0}^{Q-1}s_{q}^{2}\overline{\mathbf{c}}\left(n-q\right) \quad (28)$$

Now, taking the z-transform from both sides of Eq. (28), the FwFxLMS characteristic equation is obtained as

$$z-A\left(z\right)+\mu\sigma_{x}^{2}\sum_{q=0}^{Q-1}s_{q}^{2}z^{-q}=0 \quad (29)$$

Substituting Eq. (18) into (29) results in

$$\frac{z-1}{1-\xi z^{-1}}+\mu\sigma_{x}^{2}\sum_{q=0}^{Q-1}s_{q}^{2}z^{-q}=0 \quad (30)$$

which can be written in the standard form of

$$1+\mu\sigma_{x}^{2}\widetilde{H}\left(z\right)=0 \quad (31)$$

where

$$\widetilde{H}\left(z\right)=\frac{\left(z-\xi\right)\sum_{q=0}^{Q-1}s_{q}^{2}z^{Q-1-q}}{z^{Q+1}-z^{Q}} \quad (32)$$

As can be seen, the FwFxLMS open loop transfer function $\widetilde{H}\left(z\right)$ has one more zero (at $z=\xi$) and one more pole (at the origin) in addition to the zeros and poles of the FxLMS open loop transfer function $H\left(z\right)$. This is the main reason behind the form of $A\left(z\right)$, given in Eq. (18). In fact, filtering the weight vector in the FwFxLMS algorithm introduces a finite real zero to the open loop transfer function of the characteristic equation. The dynamic of the adaptation process, performed by the FwFxLMS algorithm, can be thus controller by localizing this zero. This is the main privilege of the FwFxLMS algorithm, compared to the FxLMS algorithm.

B. FwFxLMS Root Locus

According to the similarity between the FxLMS and FwFxLMS characteristic equations and based on the same logic, used for the derivation of FxLMS root locus rules in [9], the following rules governing on the FwFxLMS root locus can be derived.

Number of Branches : Since $\widetilde{H}\left(z\right)$ has one pole more than $H\left(z\right)$, FwFxLMS root locus has one branch more than the FxLMS root locus. Accordingly, this root locus has $Q+1$ branches, denoted by $\widetilde{B}_{1},\widetilde{B}_{2},...$and $\widetilde{B}_{Q+1}$.

Start Points : the start point of $\widetilde{B}_{1}$ locates at $z=1$ and those of $\widetilde{B}_{2},\widetilde{B}_{3},...$ and $\widetilde{B}_{Q+1}$ locate at the $z=0$, commonly.

End Points: end points of the FwFxLMS root locus locate at the zeros of $\widetilde{H}\left(z\right)$. Since $s_{0}^{2},s_{1}^{2},\ldots,s_{Q-1}^{2}$ are positive scalars, the FxLMS open loop transfer function $H\left(z\right)$ can not have any real zero to the right side of the imaginary axis (positive real zero). However, the FwFxLMS open loop transfer function $\widetilde{H}\left(z\right)$ has a real zero inside the unit circle at $z=\xi$ (since $0<\xi<1$). This is one of the main distinction between the FxLMS and FwFxLMS root loci.

Asymptotes: asymptotes of the FwFxLMS root locus originate on the real axis at the centroid point $\widetilde{x}_{A}$, given by

$$\widetilde{x}_{A}=x_{A}-\frac{\xi}{Q_{0}+1} \quad (33)$$

and form angles with respect to the real axis of

$$\widetilde{\varphi}_{k}=\varphi_{k} \qquad k=0,1,...,Q_{0} \quad (34)$$

where x_{A} is the centroid point in the FxLMS root locus and φ_{k} is the angle of the k-th asymptotes in the FxLMS root locus. For a given secondary path, FxLMS and FwFxLMS root loci have the same number of asymptotes. This is because this number equals to the difference between the poles and zeros of the open loop transfer function and for both the FxLMS and FwFxLMS characteristic equations this number equals to $Q_{0}+1$.

Departure Angles: the departure angle of the FwFxLMS root locus branches from their start points are given by

$$\widetilde{\theta}_{q}=\begin{cases}\pi, & q=1\\ \frac{2(q-1)}{Q}\pi, & q=2,3,...,Q+1\end{cases} \quad (35)$$

Real Sections: since $0<\xi<1$, the real interval of $(\xi,1)$ always belongs to the FwFxLMS root locus. However, the real interval of $(0,\xi)$ does not definitely belong to the FwFxLMS root locus. This is while the interval of $(0,1)$ belongs to the FxLMS root locus, entirely.

Breakaway Points: unlike the FxLMS root locus, the FwFxLMS root locus does not necessarily have a breakaway point close on its real section. More precisely, when ξ is set properly (not very close to the origin) the root locus has no breakaway point in the interval of $(0,1)$. However, when ξ is set close to the origin the root locus may have two breakaway point in this interval.

In the following, it is shown that if ξ holds the following inequality, the the FwFxLMS root locus has no breakaway point on the positive real axis.

$$2 - x_B - 2\sqrt{1 - x_B} < \xi < 1 \tag{36}$$

Proof: Any breakaway point in the FwFxLMS root locus should satisfy the breakaway point equation of

$$\widetilde{x}_B = \arg\left\{ \frac{\partial}{\partial z} \frac{1}{\widetilde{H}(z)} \right\} = 0 \tag{37}$$

On the other hand, from Eq. (32) it can be shown that

$$\frac{\partial}{\partial z}\frac{1}{\widetilde{H}(z)} = \frac{z^{Q-1}}{(z-\xi)^2 G^2(z)} \times \Big\{ [(Qz - Q + 1)(z-\xi) - \xi(z-1)] G(z) - \left(z^2 - z\right)(z-\xi)\acute{G}(z) \Big\} \tag{38}$$

where $G(z)$ is defined as

$$G(z) = \sum_{q=0}^{Q-1} s_q^2 z^{Q-1-q} \tag{39}$$

Now, combining Eqs. (37) and (40) gives the following equation for the FwFxLMS root locus breakaway point.

$$(Q\widetilde{x}_B - Q + 1)(\widetilde{x}_B - \xi) - \xi(\widetilde{x}_B - 1) - \left(\widetilde{x}_B^2 - \widetilde{x}_B\right)(\widetilde{x}_B - \xi)\frac{\acute{G}(\widetilde{x}_B)}{G(\widetilde{x}_B)} = 0 \tag{40}$$

If there is a breakaway point of the FwFxLMS root locus, it should be close to $z = 1$; therefor, the following assumptions can be made (similar to those made in [9] for the FxLMS root locus)

$$\widetilde{x}_B^2 - \widetilde{x}_B = (\widetilde{x}_B - 1)^2 + \widetilde{x}_B - 1 \approx \widetilde{x}_B - 1 \tag{41}$$

and

$$\frac{\acute{G}(\widetilde{x}_B)}{G(\widetilde{x}_B)} \approx \frac{\acute{G}(1)}{G(1)} \tag{42}$$

Using these two assumptions, Eq. (40) can be simplified to

$$(Q\widetilde{x}_B - Q + 1)(\widetilde{x}_B - \xi) - \xi(\widetilde{x}_B - 1) - (\widetilde{x}_B - 1)(\widetilde{x}_B - \xi)\frac{\acute{G}(1)}{G(1)} = 0 \tag{43}$$

In [9], it is shown that

$$\frac{\acute{G}(1)}{G(1)} = Q - 1 - D_{eq} \tag{44}$$

Now, substituting Eq. (44) into (43) results in

$$(1 + D_{eq})\widetilde{x}_B^2 - (2\xi + \xi D_{eq} + D_{eq})\widetilde{x}_B + \xi(1 + D_{eq}) = 0 \tag{45}$$

which can be expressed as

$$\widetilde{x}_B^2 - \left(\xi + \frac{D_{eq} + \xi}{1 + D_{eq}}\right)\widetilde{x}_B + \xi = 0 \tag{46}$$

Since $D_{eq} \gg 1$ and $0 < \xi < 1$, this equation can be approximated by

$$\widetilde{x}_B^2 - \left(\xi + \frac{D_{eq}}{1 + D_{eq}}\right)\widetilde{x}_B + \xi = 0 \tag{47}$$

As can be seen, the FxLMS breakaway point x_B, as given in Eq. (14), appears in the breakaway point equation of the FwFxLMS root locus. Thus,

$$\widetilde{x}_B^2 - (\xi + x_B)\widetilde{x}_B + \xi = 0 \tag{48}$$

Note that in the above breakaway point equation, $\widetilde{x}_B$ is the unknown variable and x_B is a known parameter. This quadratic equation has no real answer if its discriminant is negative. Thus, any value of ξ, for which there is no breakaway point on $(\xi, 1)$ in the FwFxLMS root locus, holds

$$(\xi + x_B)^2 - 4\xi < 0 \tag{49}$$

This inequality can be expanded as follows.

$$2 - x_B - 2\sqrt{1 - x_B} < \xi < 2 - x_B + 2\sqrt{1 - x_B} \tag{50}$$

It can be shown that for $x_B > 0$,

$$2 - x_B + 2\sqrt{1 - x_B} > 1 \tag{51}$$

Therefore, considering that $0 < \xi < 1$, the inequality given in Eq. (50) is simplified to the one given in Eq. (36).

C. Typical Trajectories of FwFxLMS Root Locus

From the rules described above, it can be deduced that, $\widetilde{B}_1$ always starts at $z = 1$ and moves towards the origin on the real axis, similar to the FxLMS root locus. However, in the FwFxLMS root locus, this branch may end at $z = \xi$ on the real axis without reaching a breakaway point.

Also, it can be deduced that $\widetilde{B}_2$ starts at $z = 0$ and moves towards the unit circle with a non-zero departure angle. This is while the departure angle of this branch in the FxLMS root locus is always zero. Other branches ($\widetilde{B}_3, \widetilde{B}_4, \ldots,$ and $\widetilde{B}_{Q+1}$) always start at $z = 0$ (with different departure angles) and moves towards the unit circle in order to end at the zeros of $\widetilde{H}(z)$ or approach the asymptotes.

Based on the typical trajectories in the FwFxLMS root locus, described above, it is expected that the nearest root to the unit circle locates on $\widetilde{B}_1$. Therefore, this branch contains the dominant root of the FwFxLMS characteristic equation, similar B_1 to the FxLMS characteristic equation. In the FxLMS root locus B_1 detours towards the unit circle after reaching the breakaway point; therefore, the maximum distance of the dominant root from the unit circle corresponds to the case

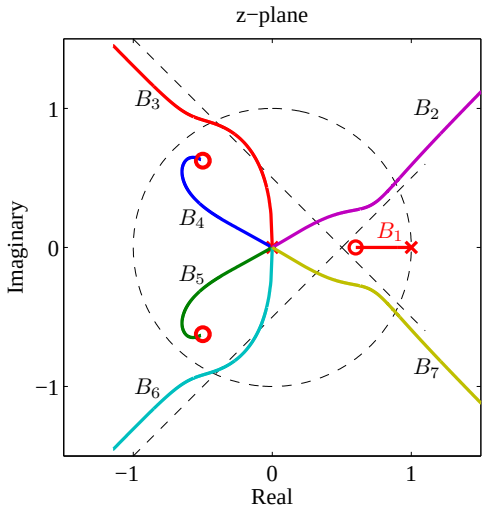

Figure 3. FwFxLMS root locus when $s_0 = s_1 = s_2 = 0$, $s_3 = s_4 = 1$ and $s_5 = 0.8$ and $\xi = 0.7$

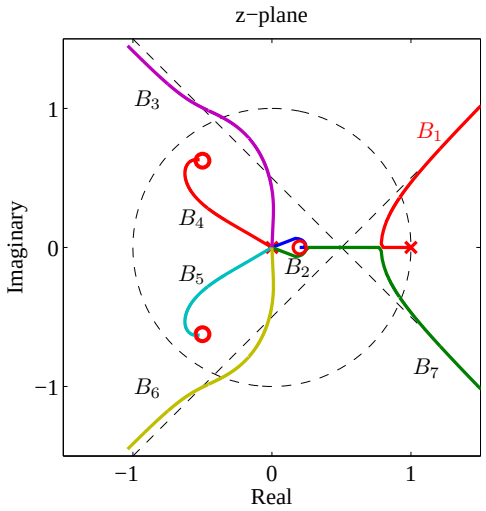

Figure 4. FwFxLMS root locus when $s_0 = s_1 = s_2 = 0$, $s_3 = s_4 = 1$ and $s_5 = 0.8$ and $\xi = 0.2$

that the root locates on the breakaway point. However, in the FwFxLMS root locus there is no breakaway point and, therefore, the root moving on $\widetilde{B}_1$ can getting closer to the origin (until it reaches the branch end point at $z = \xi$). As a result, the dominant root of the characteristic equation (which id the dominant pool of the process) can be pushed towards the origin so that the dynamic of the FwFxLMS adaptation process becomes faster than that of the FxLMS.

D. Examples

Figure 3 shows the FwFxLMS root locus for the system described in Section 2 when ξ is set to 0.7. As can be seen, there is no breakaway point on the trajectory of the dominant root (branch B_1) and, therefore, this root can becomes closer to the origin (compared to the FxLMS root locus shown in Figure 2).

Figure 4 shows another example of the FwFxLMS root locus when ξ is set to 0.2. This is while the minimum level for ξ can be obtained from Eq. (36) as 0.25. In this case, since the open loop zero locating at ξ is too close the origin, it attracts two of branches departing from the origin. In this case, the existence of two breakaway points on the real interval between ξ and 1 is essential. Consequently, the general shape of the root locus is more similar to that of the FxLMS. As a conclusion, setting ξ to a number smaller than 1 causes the dominant root to become closer to the origin (leading to faster dynamics), compared to the FxLMS root locus; however, this parameter should not be set smaller that the proposed minimum level because it causes a breakaway point close to $z = 1$ on the root locus.

IV. Computer Simulation

In order to verify the performance of the FwFxLMS algorithm in ANC systems, several simulation experiments have been conducted in MATLAB® environment. In all of these experiments, environmental noise is a computer-generated white noise with a variance of $\sigma_x^2 = 1$. The secondary path, used in the computer simulation, is similar to the one introduced in the example of Sections 2 and 3. A low-pass filter of length 18 is used as the primary path; and the ANC controller is implemented using a transversal filter of length $L = 15$. The results are obtained by averaging over 100 different simulation runs with independent sequences of noise.

Figure **??** shows the mean square of the error signal $e(n)$ (referred to as the MSE), obtained by averaging over all simulation runs results. As can be seen in this figure, the MSE function obtained by FxLMS algorithm has the slowest convergence, compared to those obtained by the FwFxLMS algorithm. According to this figure, When ξ is set to 0.7, then the convergence speed of the MSE significantly becomes faster. In this case, the dynamic of the adaptation process corresponds to the root locus plot shown in Figure 3. When ξ is set to still smaller number, then the convergence speed of the MSE function becomes even faster. For example, the MSE function obtained by settoing $\xi = 0.6$, shown in Figure 3. However, it is expected from Eq. (36) that setting ξ bellow 0.25 causes the MSE function becomes slower. For example, the MSE function obtained by setting $\xi = 0.2$ is shown in Figure **??**. As can be seen, the convergence speed is still faster than the FxLMS; however, the improvment, caused by reducing ξ, cannot be seen any more. In this case, the dynamic of the adaptation process corresponds to the root locus plot shown in Figure 4. This behaviour is in an excellent agreement with the theoretical results obtained in Section 3.2.

V. Conclusion

The root locus analysis of the adaptation process, performed by the FxLMS algorithm in ANC systems, leads to obtain interesting ideas for the dynamic control of this process. The FxLMS algorithm has no control mechanism over the locations of its poles. However, the proposed FwFxLMS algorithm

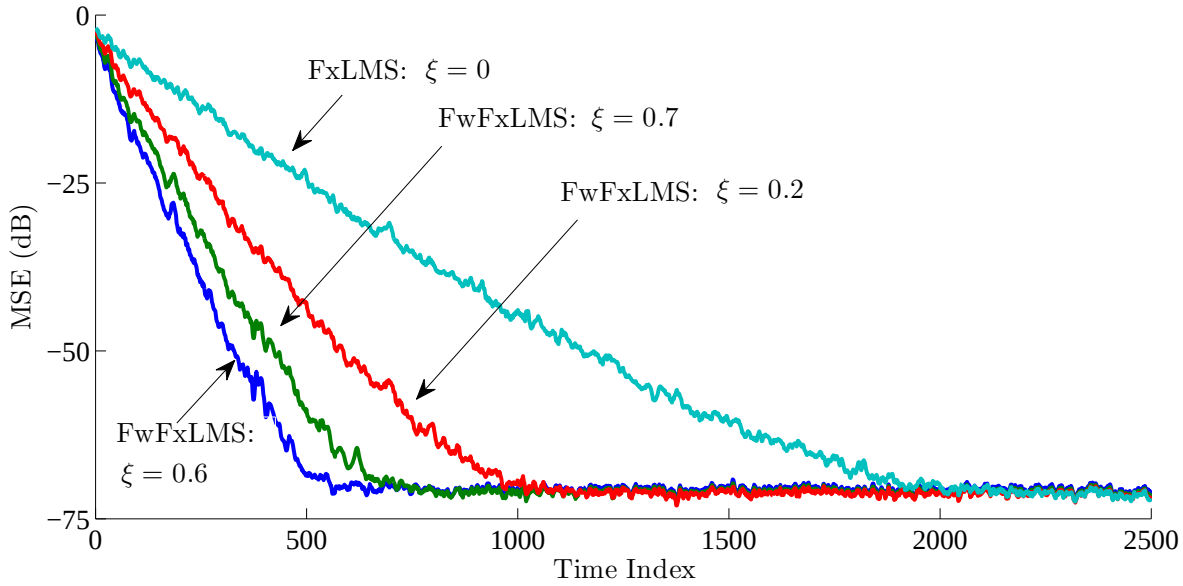

Figure 5. Variatins of MSE function obtained by using FxLMS and FwFxLMS algorithms

provide with a parameter which enable us to localize the dominant pole of the adaptation process. The results shows that if this parameter adjusts properly, then the dominant root of the adaptation process can get closer to the origin and, thereby, the MSE function can converges to its steady-state level faster.

REFERENCES

[1] B. Widrow, J. Glover, J. McCool, J. Kaunitz, C. Williams, R. Hearn, J. Zeidler, J. Eugene Dong, and R. Goodlin, "Adaptive noise cancelling: principles and applications," *Proceedings of the IEEE*, vol. 63, no. 12, pp. 1692–1716, December 1975.

[2] D. R. Morgan, "An analysis of multiple correlation cancellation loops with a filter in the auxiliary path," *Acoustics, Speech, and Signal Processing, IEEE International Conference on ICASSP '80.*, pp. 457–461, April 1980.

[3] J. C. Burgess, "Active adaptive sound control in a duct: computer simulation," *Journal of the Acoustical Society of America*, vol. 70, pp. 715–726, 1981.

[4] G. E. Warnaka, L. A. Poole, and J. Tichy, "Active acoustic attenuators," *U.S. Patent 4473906*, 1984.

[5] L. J. Eriksson, "Recursive algorithms for active noise control," *International Symposium of Active Control of Sound and Vibration*, pp. 137–146, 1991.

[6] S. M. Kuo and D. R. Morgan, *Active noise control systems: algorithms and DSP implementations*. New York, NY, USA: Wiley Interscience, 1996.

[7] S. J. Elliott, *Signal Processing for Active Control*. San Diego, CA.: Academic Press, 2001.

[8] B. Widrow, D. Shur, and S. Shaffer, "On adaptive inverse control," in *Proceeding of the 15th Asilomar Conference on Circuits, Systems and Computers*, November 1981, pp. 185–189.

[9] I. T. Ardekani and W. Abdulla, "On the stability of adaptation process in active noise control systems," *Journal of Acoustical Society of America*, vol. 129, no. 1, pp. 173–184, 2011.

[10] ——, "Convergence analysis of active noise control systems using root locus theory," *Proceedings of 2009 Asia Pacific Signal and Information Processing Association Annual (APSIPA) Summit and Conference, Biopolis, Singapore*, pp. 141–144, 14-17 December, 2010.

[11] E. Bjarnason, "Analysis of the filtered-x LMS algorithm," *Speech and Audio Processing, IEEE Transactions on*, vol. 3, no. 6, pp. 504–514, November 1995.